Supercritical Carbon Dioxide-Assisted Dispersion of Sodium Benzoate in Polypropylene and Crystallization Behavior of the Resulting Polypropylene

Bin Li,[1] Guo-Hua Hu,[2,3] Gui-Ping Cao,[1] Tao Liu,[1] Ling Zhao,[1] Wei-Kang Yuan[1]

[1]*UNILAB Research Center of Chemical Reaction Engineering, State Key Laboratory of Chemical Engineering, East China University of Science and Technology, Shanghai 200237, China*
[2]*Laboratory of Chemical Engineering Sciences, CNRS-ENSIC-INPL, BP 20451, 54001 Nancy Cedex, France*
[3]*Institut Universitaire de France, Maison des Universités, 75005 Paris, France*

Received 13 July 2005; accepted 8 March 2006
DOI 10.1002/app.24559
Published online in Wiley InterScience (www.interscience.wiley.com).

ABSTRACT: This work aimed at studying the efficiency of the use of supercritical carbon dioxide ($scCO_2$) as a swelling agent to disperse sodium benzoate (NaBz), a nucleating agent, in polypropylene (PP), on the one hand; and the crystallization behavior of the resulting PP, on the other hand. Under $scCO_2$, the NaBz was uniformly dispersed in the PP at a nanometer scale. The use of ethanol or acetone as a cosolvent further increased its state of dispersion and its mass uptake in the PP. Isothermal and nonisothermal crystallization kinetics indicated that the PP with the NaBz being dispersed in it under $scCO_2$ had a much higher crystallization rate than that of the pure PP or the PP with the NaBz being dispersed in it by a conventional melt compounding process. The size of the PP crystallites was also much smaller when the NaBz was dispersed at a nanometer scale. © 2006 Wiley Periodicals, Inc. J Appl Polym Sci 102: 3212–3220, 2006

Key words: supercritical carbon dioxide; polypropylene; sodium benzoate; dispersion

INTRODUCTION

As a general-purpose polymer, polypropylene (PP) has various excellent properties such as mechanical rigidity, thermal and chemical resistance, ease of processing, and recycling. Many properties of PP depend very much on its crystallinity and crystalline morphology. Nowadays processing techniques require shorter and shorter cycle times. The addition of nucleating agents to PP accelerates the crystallization process and therefore shortens the cycle time.[1–4]

Sodium benzoate (NaBz) has frequently been used as a flavoring or antimicrobial agent.[5] It may also be used as a nucleating agent for PP.[6–9] This is because its melting point is high (439°C), is insoluble in the PP melt at typical processing temperatures, and crystallizes much earlier than PP.[10] A nucleating agent like NaBz is usually added to PP by extrusion compounding. The driving force for dispersion is a mechanical force the extruder imparts to the NaBz particles. Under such conditions, the state of dispersion of the NaBz is not optimal.

Supercritical fluids (SCFs) have been gaining popularity in polymer processing.[11–17] Carbon dioxide has by far been the most frequently used SCF candidate owing to its unique properties: nonflammable, nontoxic, relatively inexpensive, relatively easy to reach supercritical conditions, etc. The aim of this work is two-folds. First, we study the extent to which the NaBz can be dissolved in supercritical carbon dioxide ($scCO_2$) and then in PP under $scCO_2$. Since the NaBz is a salt bearing a polar group, we test the efficiency of using a cosolvent at enhancing its solubility and therefore its mass uptake in the apolar PP. Second, we compare the isothermal and nonisothermal crystallization kinetics of PP in which the NaBz is dispersed by different processes: conventional melt compounding, $scCO_2$-assisted dispersion, and $scCO_2$/cosolvent-assisted dispersion.

EXPERIMENTAL

Penetration of NaBz to PP

A commercial isotactic polypropylene (PP0) was used in this study. It was provided by Shanghai Petrochemi-

Correspondence to: G.-H. Hu (hu@ensic.inpl-nancy.fr) or W.-K. Yuan (wkyuan@ecust.edu.cn).

Contract grant sponsor: International cooperation project; contract grant number: 2001CB711203.
Contract grant sponsor: Shanghai Science and Technology Commission (SSTC) for Nanotechnology researches; contract grant number: 0552nm039.
Contract grant sponsor: NSFC/PetroChina joint project for multiscale methodology; contract grant number: 20490200.

TABLE I
Characteristics of the PP and NaBz Used in This Work

Material	Property	Value
PP0	Melt flow index (g/10 min, 230°C)	16
	Polydispersity index	5.1
	M_w (g/mol)	188,700
	T_g (°C)	−5
NaBz	Density (g/cm^3)	1.46
	Formula mass (g/mol)	144.1
	Average particle size (μm)	200
	Melting point (°C)	439

cal Company, China, in a powdery form under the tradename Y1600. About 15 g of the PP0 powder was first molten in an oven at 200°C and then pressed to a film of 0.3-mm thickness using a press under 10 MPa. The film was then cut into pieces of 1 mm × 3 mm × 0.3 mm. The latter were refluxed in acetone for 24 h to remove impurities and then dried at 100°C for 2 h. The NaBz was purchased from Shanghai Chemical Reagent Company, China. Table I gathers some of the characteristics of the PP0 and NaBz.

Figure 1 shows the experimental apparatus used for the penetration of the NaBz to the PP0 under scCO$_2$. It was mainly composed of a gas cylinder, a high-pressure reactor (Parr Instrument, Co.), a gas booster (Haskel International), a digital pressure gauge, an electrical heating bath, and valves and fittings of different kinds. All the metallic parts in contact with chemicals were made of stainless steel. The apparatus was tested up to 40 MPa. It had a volume capacity of 500 mL.

PP films were placed in the high-pressure cell together with 1 wt % of the NaBz. The system was then purged with CO$_2$. When it reached a desired temperature of 60°C (an optimal one for the penetration of nucleating agent according to a previous work[17]), CO$_2$ was charged till a desired pressure was attained. The penetration process lasted 4 h. Thereafter the high-pressure cell was rapidly depressurized. It was then cooled down, opened up, and the PP films were taken out. A gravimetric technique[18] was used to measure the mass uptake of the NaBz in the PP films. A high-precision electrical balance (BP211D, Sartorius, Germany) was used for that purpose. It had an accuracy of within ±0.01 mg. A scanning electron microscope (SEM) of type JEOL/EO JSM-6360 was used to visualize the state of dispersion of the NaBz in the PP.

Ethanol and acetone were used as cosolvents for the penetration of the NaBz in the PP0. They were purchased from Shanghai Reagent Company and their purities were above 99.8%. When prescribed pressure and temperature were reached, 20 mL of ethanol or acetone (0.05 wt % with respect to the PP0) was added to the system using a high-pressure advection pump (LB-10, Beijing Satellite Instrument Co., China).

Morphology of the PP crystalline phases

The morphology of the PP crystalline phases was studied using an optical polarized microscope (BX51, Olympus, Japan) equipped with a hot stage (THMS 600, Linkam, Great Britain). A PP sample was sandwiched between two microscope cover glasses, heated to 200°C, kept at that temperature for 5 min, and then cooled down to 140°C with a cooling rate of 100°C/min for isothermal crystallization and crystalline morphology observations.

Crystallization analysis

A differential scanning calorimeter of type Perkin–Elmer Pyris Diamond DSC was used to study the crystallization behavior of PP samples. Five types of sam-

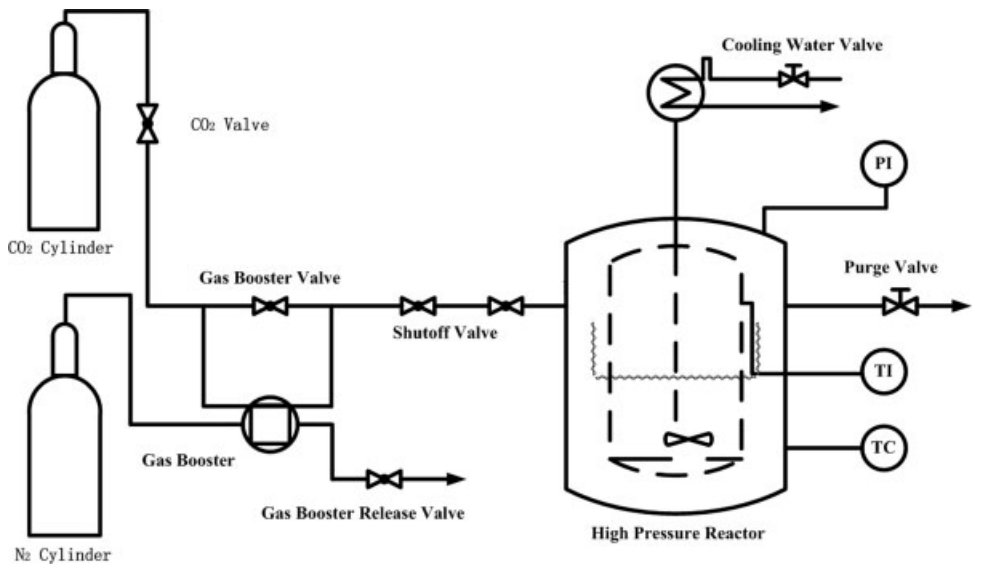

Figure 1 Schematic of the apparatus used for the scCO$_2$-assisted penetration of the NaBz in the PP0.

TABLE II
PP Samples Used in This Work

Sample	Preparation technique	Mass percentage of NaBz in PP
PP0	Virgin	0
PP1	NaBz was dispersed in the PP0 by a conventional compounding technique	0.12
PP2	NaBz was dispersed in the PP0 by a conventional compounding technique	0.85
PP3	NaBz was incorporated in the PP0 under $scCO_2$	0.12
PP4	NaBz was incorporated in the PP0 under $scCO_2$ and in the presence of ethanol as a co-solvent (0.05 wt% with respect to the PP0)	0.85
PP5	NaBz was incorporated in the PP0 under $scCO_2$ and in the presence of acetone as a co-solvent (0.05 wt% with respect to the PP0)	1.65

ples (PP0–PP4) were studied, as shown in Table II. All of them were extruded and pelletized with a twin-screw extruder (SJSH-30) for DSC analysis.

In a typical isothermal crystallization experiment, about 5 mg of a PP sample in the form of pellets was heated up to 200°C and kept at that temperature for 10 min to remove any thermal history. It was then cooled down to a prescribed crystallization temperature. For the nonisothermal crystallization, the crystallization thermograms were obtained by cooling the sample at different cooling rates ranging from 1 to 20°C/min. For the isothermal crystallization, the crystallization temperature ranged from 110 to 135°C and the cooling rate was 100°C/min.

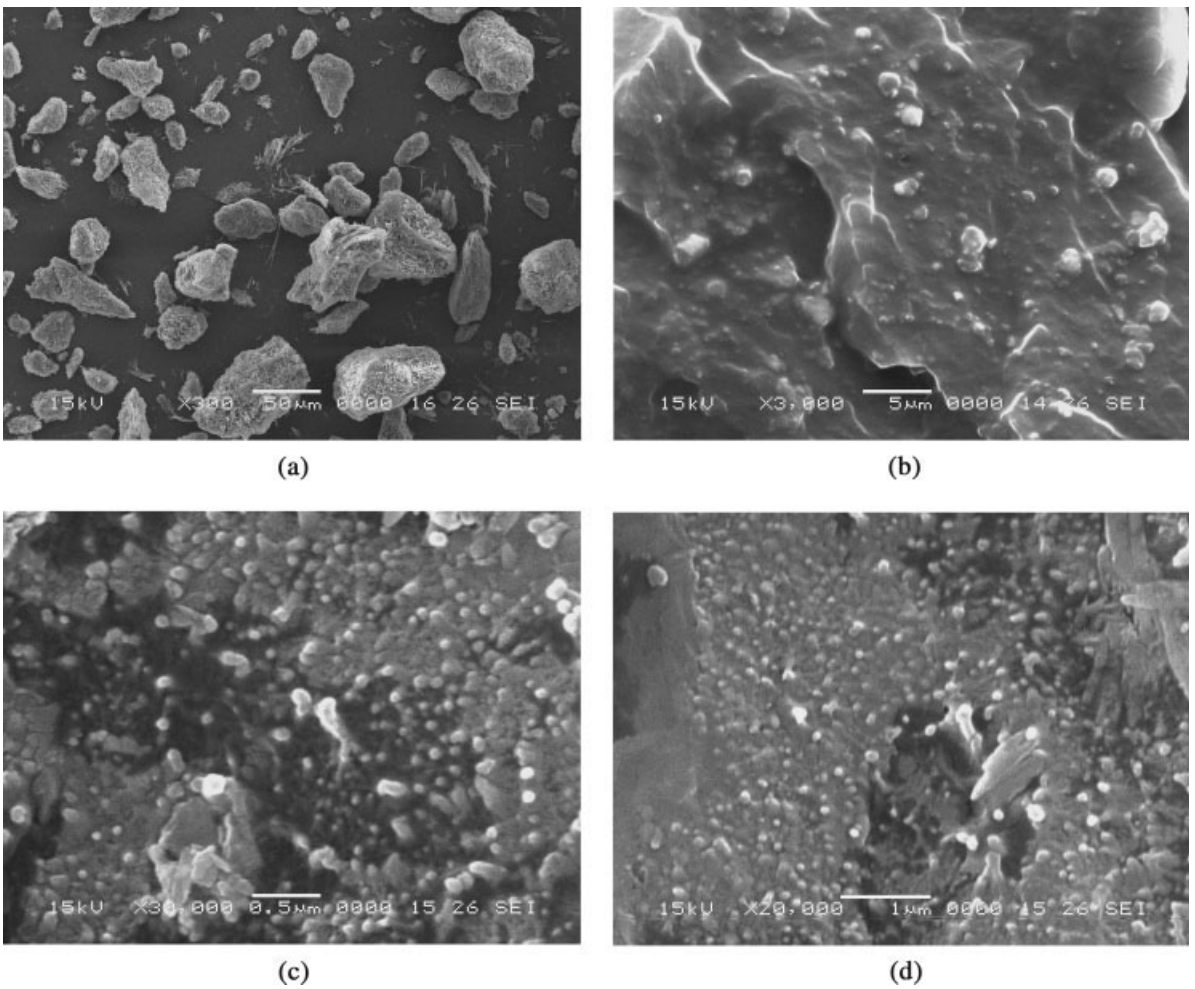

Figure 2 SEM images showing the morphology of the NaBz particles alone and the state of dispersion of the latter in PP3, PP4, and PP5. The penetration process was carried out under the following conditions: temperature = 60°C, CO_2 pressure = 8.3 MPa, and time = 4 h. When a cosolvent was used, its amount was 0.05 wt % of the PP. (a) NaBz alone, (b) PP3, (c) PP4, and (d) PP5.

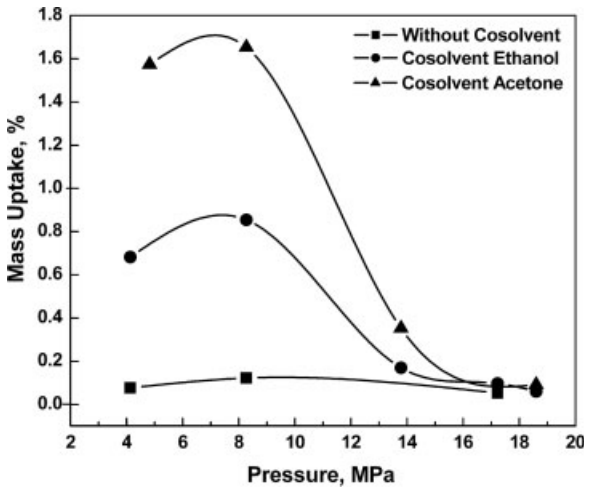

Figure 3 Effect of the scCO$_2$ pressure on the mass uptake of the NaBz in the PP0. The penetration process was carried out under the following conditions: temperature = 60°C, CO$_2$ pressure = 8.3 MPa, and time = 4 h.

A nonisothermal crystallization thermogram showed the variation of the enthalpy of crystallization as a function of temperature under a given cooling rate. On the other hand, an isothermal crystallization thermogram showed the variation of the enthalpy of crystallization as a function of time at a given crystallization temperature.

The crystallinity of the PP samples was calculated by the following equation:[3,19]

$$X_c = \frac{\Delta H(t)}{\Delta H_f} \quad (1)$$

where $\Delta H(t)$ is the enthalpy of crystallization at time t, and ΔH_f the enthalpy of fusion of a 100% crystalline PP (209 J/g). The relative crystallinity was calculated by:[20–22]

$$V_c(t) = \frac{X(t)}{X_{c\to\infty}} = \int_0^t (dH/dt)dt \Big/ \int_0^\infty (dH/dt)dt \quad (2)$$

where $X_{c\to\infty}$ is the crystallinity at equilibrium and dH/dt is the enthalpy variation rate.

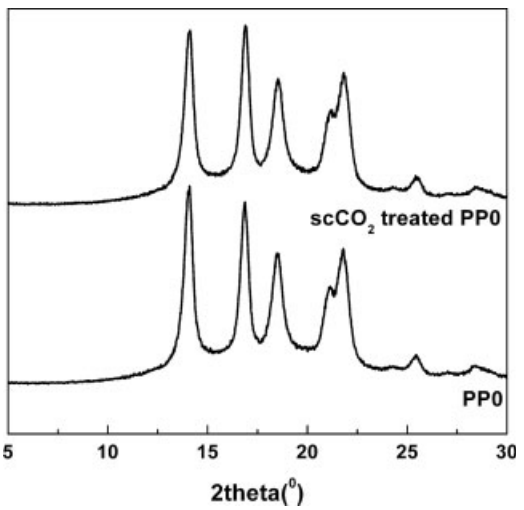

Figure 4 X-ray diffractograms of PP0 and PP0 treated with scCO$_2$ (temperature = 60°C, CO$_2$ pressure = 8.3 MPa, and time = 4 h).

RESULTS AND DISCUSSION

Penetration and mass uptake of the NaBz in the PP0

Penetration of the NaBz into the PP0 matrix proceeded under scCO$_2$ with and without the presence of a cosolvent. The SEM images in Figure 2 show the morphology of the NaBz alone and its state of dispersion in PP3, PP4, and PP5. It is seen that the size of the NaBz particles was greatly reduced when they penetrated into PP matrix under scCO$_2$, especially when ethanol

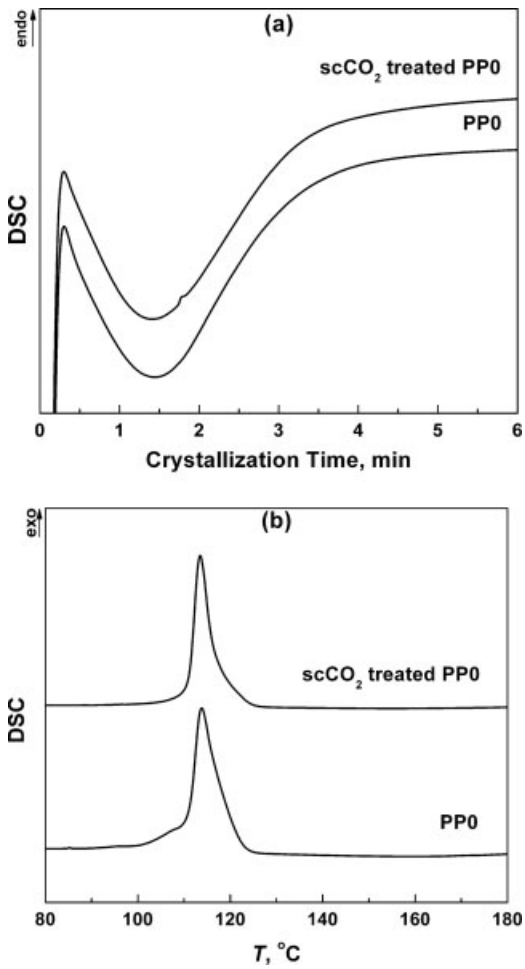

Figure 5 Thermograms of PP0 and PP0 treated with scCO$_2$ (temperature = 60°C, CO$_2$ pressure = 8.3 MPa, and time = 4 h) for (a) isothermal (crystallization temperature, 120°C) and (b) nonisothermal crystallization (cooling rate, 10°C/min).

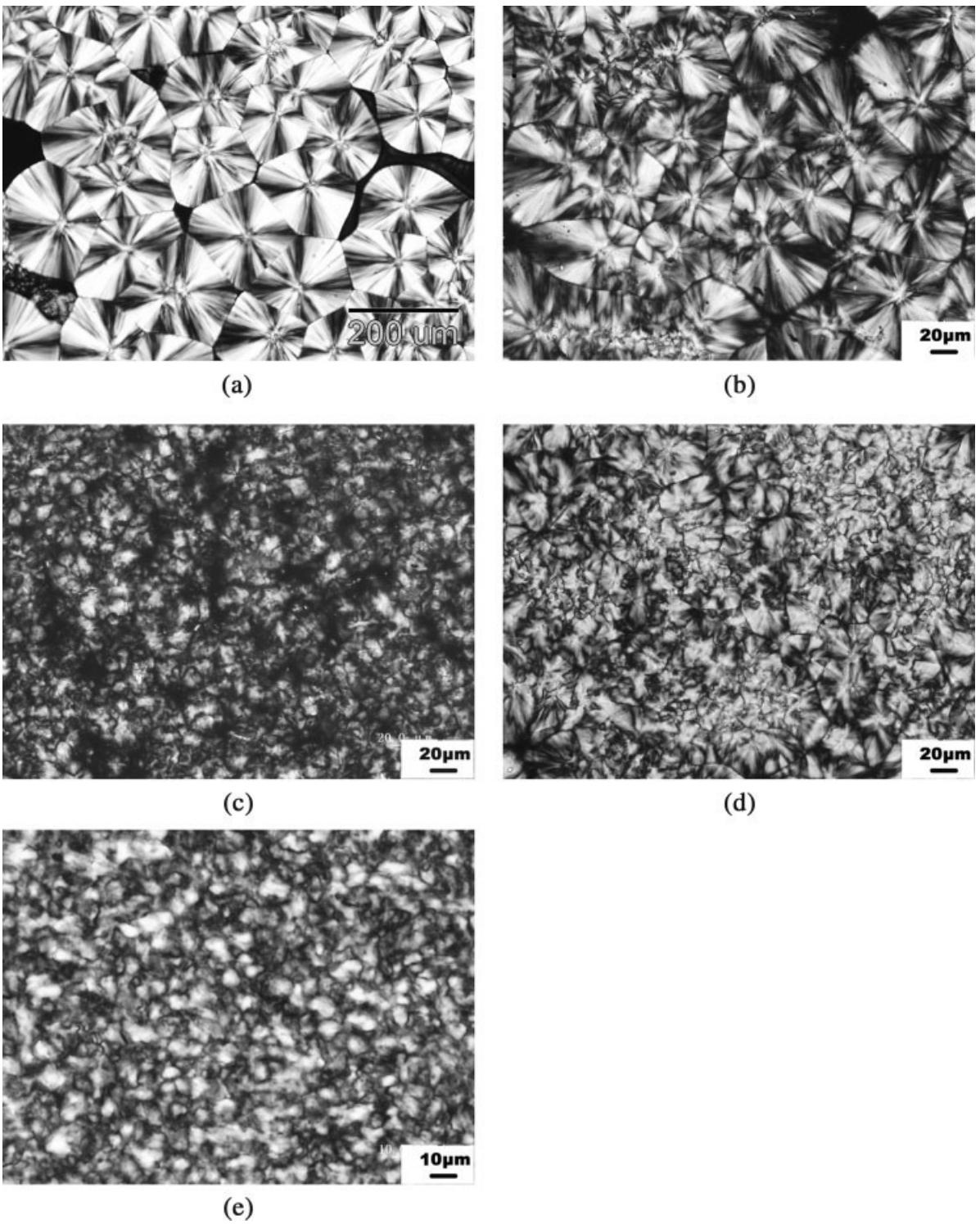

Figure 6 Optical microscopic photographs of the PP samples crystallized at 140°C for an hour after having been kept at 200°C for 10 min and then cooled down to 140°C with a cooling rate of 100°C/min. (a) PP0, (b) PP1, (c) PP2, (d) PP3, and (e) PP4.

was added. Moreover, the addition of the cosolvent seemed to lead to more homogeneous dispersion of the NaBz particles in the PP.

Figure 3 compares the mass uptake of the NaBz in the PP0 obtained under three different penetration conditions. The mass uptake was always very low (of the order of 0.1 wt % only) when the NaBz penetrated the PP0 under $scCO_2$ without a cosolvent, irrespective of the $scCO_2$ pressure (4–18 MPa). When a cosolvent (acetone or ethanol) was used, the mass uptake became much higher, reaching a maximum of 1.65 wt %. This significant increase in the mass uptake could be

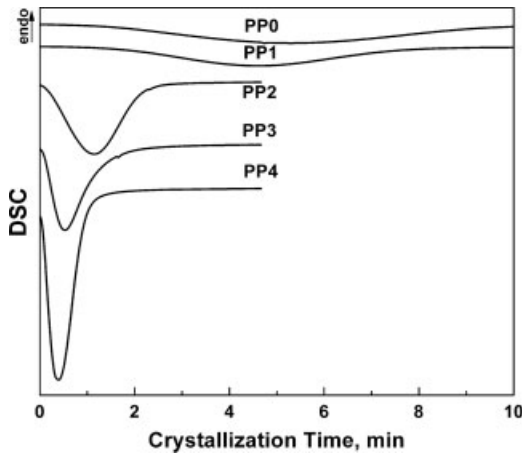

Figure 7 Heat flow versus time for the isothermal crystallization at 130°C.

explained by an enhanced solubility of the NaBz in the scCO$_2$ when a cosolvent was added. Acetone was clearly much more efficient in increasing the mass uptake of the NaBz than ethanol. Moreover, the mass uptake depended very much on the scCO$_2$ pressure too. Apparently there was an optimum for the scCO$_2$ pressure corresponding to a maximum of the mass uptake of the NaBz in the PP0. It was somewhere between 7 and 9 MPa for both cosolvents. That optimum could be related to the partitioning of the NaBz between the scCO$_2$ and PP0 matrix. The solubility of the NaBz in the scCO$_2$ increased rapidly with increasing scCO$_2$ pressure. When the latter was very high, it might be that the NaBz was partitioned more in the scCO$_2$ than in the PP0 matrix. Moreover, during the rapid CO$_2$ depressurization process when the initial CO$_2$ was high, some of the NaBz might leach out from the PP0 matrix further contributing to a decrease in the mass uptake of the NaBz.

Morphology of the PP crystalline phases

Before we will discuss on the effect of the NaBz on the crystallization behavior and crystalline structures of the PP0, it is important to check whether or not scCO$_2$ had an effect on them. Figure 4 compares the X-ray diffractograms between the PP0 and the PP0 treated with scCO$_2$ without NaBz and under the following conditions: temperature = 60°C, CO$_2$ pressure = 8.3 MPa, and time = 4 h. The two diffractograms were virtually the same, indicating that the crystalline structures of the PP0 did not change after the treatment with scCO$_2$ under the above conditions. This is further confirmed by their isothermal and nonisothermal DSC traces in Figure 5. Again, both the PP0 and the PP0 treated with scCO$_2$ under the above conditions had the same isothermal and nonisothermal crystallization curves, and thus the same crystallization behavior. In short, under the above conditions, scCO$_2$ alone did not impart any noticeable effect on the crystalline structures of the PP0.

Figure 6 compares, in a qualitative manner, the crystalline morphologies of PP0, PP1, PP2, PP3, and PP4. As expected, the size of the PP crystallites followed the order: PP0 > PP1 > PP2 > PP3 > PP4. Those results were in agreement with both the state of dispersion and the amount of the NaBz in the PP0 described above (see Table II and Fig. 2). It is interesting to recall that the PP1 and PP3 contained both the same amount of the NaBz, i.e., 0.12 wt %. The only difference was that in the former case the NaBz was dispersed in the PP0 by a conventional melt compounding process whereas in the latter case, it was done under scCO$_2$. Thus the fact that the size of crystallites of the PP3 was smaller than that of the PP1 by more than an order of magnitude was a strong piece of evidence supporting the advantage of using scCO$_2$ for finely dispersing the NaBz in the PP0. This is further confirmed by comparing PP2 and PP4. They also contained the same but larger amount of NaBz, i.e., 0.85 wt %.

Isothermal crystallization kinetics

Figures 7 and 8 show the variation of the heat flow and that of the relative crystallinity as a function of the crystallization time, respectively. The results show that the presence of the NaBz greatly accelerated the crystallization process of the PP0, confirming that the NaBz did act as a nucleating agent for the PP0. The crystallization rate followed the order: PP0 < PP1 < PP2 < PP3 < PP4, as expected.

The isothermal crystallization half-time, $t_{1/2}$, characterizes the time at which 50% of the total crystallization process has completed. A smaller value of $t_{1/2}$ corresponds to a more rapid crystallization process. Figure 9 compares the values of $t_{1/2}$ for the four PP samples. Again as expected, the value of $t_{1/2}$ followed the order: PP0 > PP1 > PP2 > PP3 > PP4.

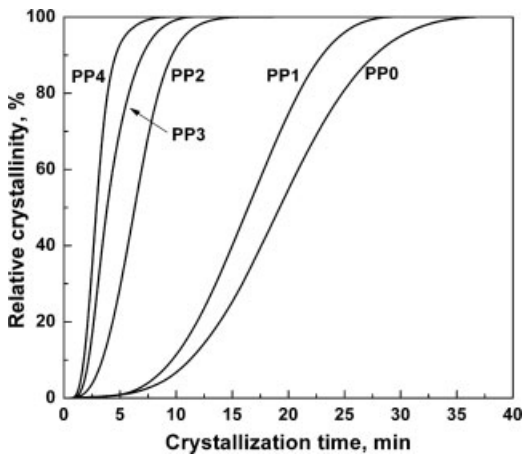

Figure 8 Relative crystallinity versus time during the isothermal crystallization at 130°C.

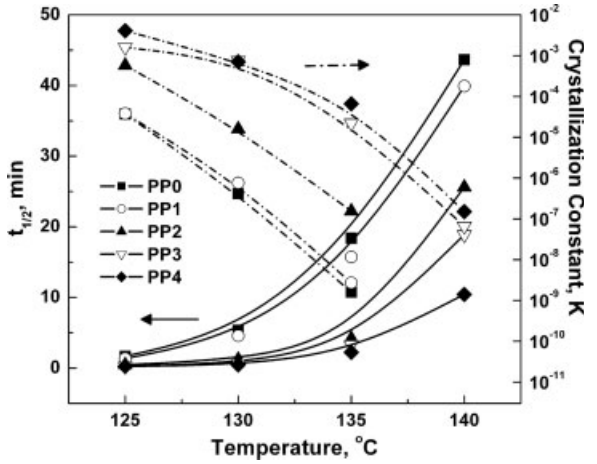

Figure 9 Isothermal crystallization half-time and crystallization constant of the PP samples as a function of the crystallization temperature.

The kinetics of the isothermal crystallization is often described by the modified Avrami equation:[3–5,10,23–28]

$$1 - X_t = \exp(-kt^n) \tag{3}$$

where X_t is the relative volume-fraction crystallinity at the crystallization time t, k is a crystallization kinetic constant, and n is the Avrami exponent whose value depend on the nucleation mechanism and the form of the growing crystals.

The above equation can also be written in the following double logarithm form:

$$\ln(-\ln(1 - X_t)) = \ln k + n \ln t \tag{4}$$

TABLE III
Isothermal Crystallization Kinetic Parameters of PP0, PP1, PP2, PP3, and PP4

Sample	Temperature (°C)	n	K	$t_{1/2}$ (min)
PP0	120	2.5	1.2×10^{-4}	0.55
	125	2.2	3.7×10^{-5}	1.67
	130	2.5	4.1×10^{-7}	5.34
	135	2.9	1.6×10^{-9}	18.38
PP1	120	2.5	2.4×10^{-4}	0.42
	125	2.3	3.8×10^{-5}	1.34
	130	2.5	7.6×10^{-7}	4.57
	135	2.8	2.7×10^{-9}	15.73
PP2	120	2.4	1.8×10^{-3}	0.224
	125	2.2	5.8×10^{-4}	0.451
	130	2.5	1.6×10^{-5}	1.20
	135	2.7	1.6×10^{-7}	4.19
PP3	125	2.3	1.6×10^{-3}	0.26
	130	1.8	7.6×10^{-4}	0.66
	135	2.0	2.2×10^{-5}	3.29
	140	2.4	6.6×10^{-8}	15.92
PP4	125	2.0	4.1×10^{-3}	0.24
	130	2.1	7.1×10^{-4}	0.45
	135	1.9	6.6×10^{-5}	2.24
	140	2.5	1.5×10^{-7}	10.42

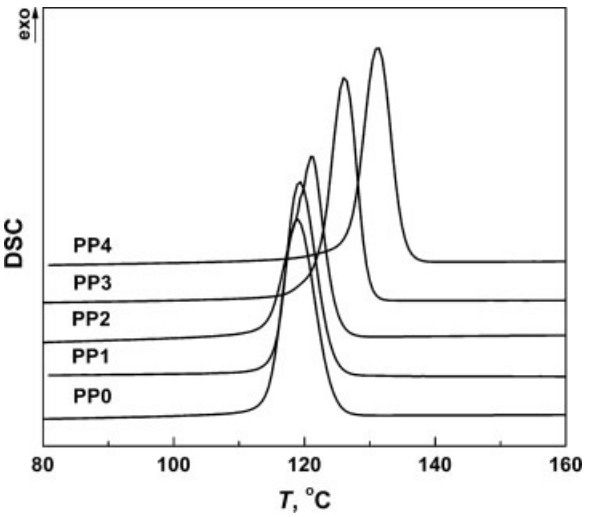

Figure 10 Heat flow versus temperature during the nonisothermal crystallization of the PP samples at a cooling rate of 5°C/min.

A plot of $\ln(-\ln(1 - X_t))$ versus $\ln t$ yields both the value of the Avrami exponent n (slope of the straight line) and that of the crystallization kinetic constant k (intersection with the coordinate). In principle, the Avrami parameter n is 3 for a spherical three-dimensional crystallization process with a heterogeneous nucleation mechanism. Its exact value depends on combined nucleation modes, secondary crystallization, intermediate dimensionality of crystal growth, etc. Table III gathers the values of the crystallization kinetic parameters (n, k, and $t_{1/2}$) for PP0, PP1, PP2, PP3, and PP4 in Table II. The values of n followed the order: PP0 $\approx$ PP1 $\approx$ PP2 $>$ PP3 $\approx$ PP4. The fact that the values of n of the PP3 and PP4 were smaller than those of PP0, PP1, and PP2 could be explained as follows. When the

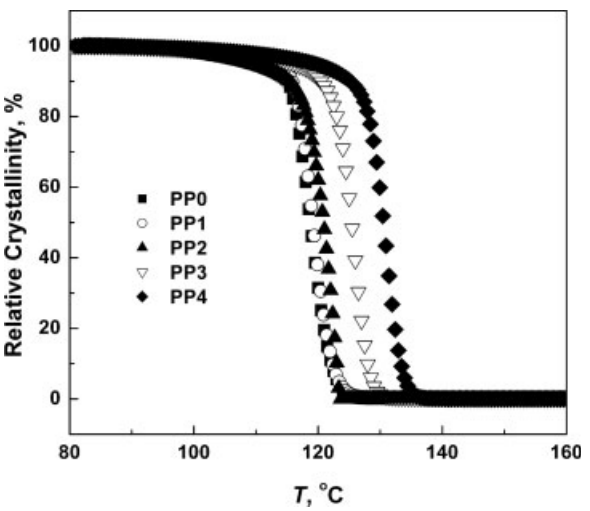

Figure 11 Relative crystallinity of the PP samples at a cooling rate of 5°C/min.

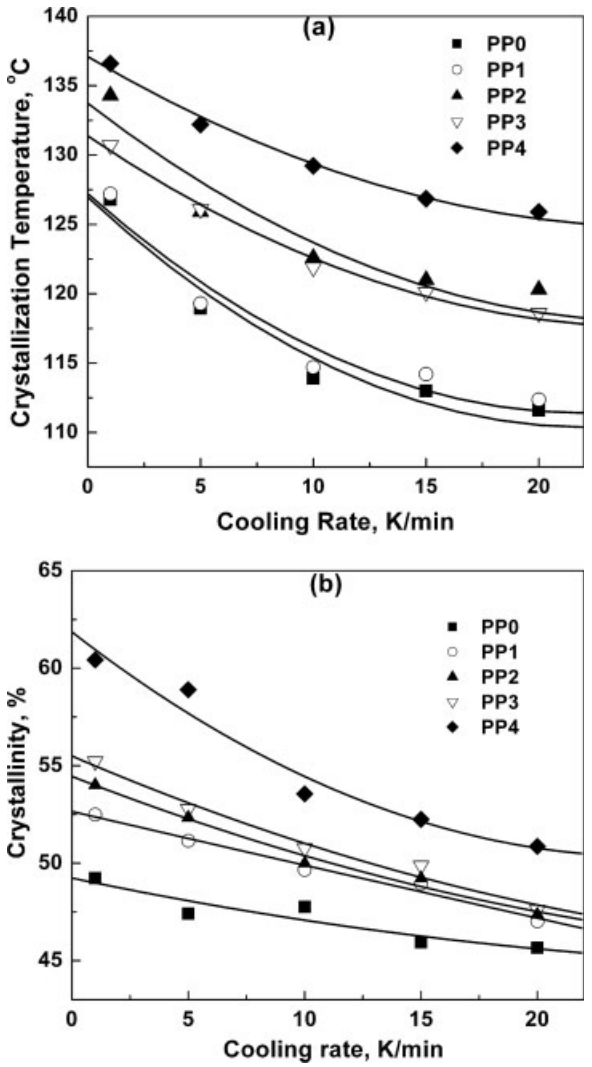

Figure 12 Nonisothermal crystallization behavior of the PP samples as a function of the cooling rate. (a) Crystallization temperature and (b) crystallinity.

NaBz was dispersed at a nanometer scale, the growth of spherulites could be more constrained because of a much larger number of nucleating sites and consequently a much smaller spacing between the growing spherulites. Thus the values of n were smaller. Figure 9 shows that at a given crystallization temperature the value of the crystallization rate constant k followed the logic order: PP0 < PP1 < PP2 < PP3 < PP4.

Nonisothermal crystallization kinetics

The results of the nonisothermal crystallization kinetics of PP0, PP1, PP2, PP3, and PP4 were in line with those of their isothermal crystallization kinetics. For example, Figures 10 and 11 show the variation of the heat flow and relative crystallinity as a function of temperature at a cooling rate of 5°C/min, respectively. As expected, the temperature at which crystallization started to proceed was the highest for the PP4 and the lowest for the PP0. The crystallization temperature, T_c, defined as a temperature at which the crystallization rate was the maximum, followed the order: PP0 < PP1 < PP2 < PP3 < PP4.

Figure 12 shows the effect of the cooling rate on the recrystallization temperature and crystallinity, respectively, for PP0, PP1, PP2, PP3, and PP4. Over the entire cooling rate range, both the recrystallization temperature and crystallinity followed the order: PP0 < PP1 < PP2 < PP3 < PP4. Moreover, they both decreased with increasing cooling rate. This is because a higher cooling rate corresponded to a shorter time available for polymer chains to crystallize.

CONCLUSIONS

This paper has reported on the feasibility and potential advantages of using scCO$_2$ as a swelling agent for assisting in the penetration and dispersion of NaBz, a nucleating agent, in PP. Under scCO$_2$, the NaBz successfully penetrated and was then finely dispersed in the PP, especially when a cosolvent like acetone or ethanol was used. In the latter case, the dispersion of the NaBz in the PP reached a nanometer scale, which was not possible otherwise by a conventional melt compounding process. Moreover, the mass uptake of the NaBz in the PP was much higher. Isothermal and nonisothermal crystallization kinetics showed that the NaBz acted as a very good nucleating agent. Its nucleating performance was much better when it was dispersed in the PP at a nanometer scale. The crystallization rate and crystallization temperature were much higher and the size of crystallites much smaller.

References

1. Xu, T.; Lei, H.; Xie, C. S. Mater Des 2003, 24, 227.
2. Feng, Y.; Jin, X.; Hay, J. N. J Appl Polym Sci 1998, 69, 2089.
3. Phillips, R.; Manson, J. E. J Polym Sci Part B: Polym Phys 1997, 35, 875.
4. Kim, C. Y.; Kim, Y. C.; Kim, S. C. Polym Eng Sci 1993, 33, 1445.
5. Oestergaard, E. Acta Odontol Scand 1994, 52, 335.
6. Jang, G. S.; Cho, W. J.; Ha, C. S. J Polym Sci Part B: Polym Phys 2001, 39, 1001.
7. Zhu, P. W.; Edward, G. Macromolecules 2004, 37, 2658.
8. Zhang, J. L. J Appl Polym Sci 2004, 93, 590.
9. Nagarajan, K.; Levon, K.; Myerson, A. S. J Therm Anal Calorim 2000, 59, 497.
10. Wunderlich, B. Macromolecular Physics, Vol. 2; Academic Press: New York, 1976.
11. Tomasko, D. L.; Li, H. B.; Liu, D. H.; Han, X. M.; Wingert, M. J.; Lee, L. J.; Koelling, K. W. Ind Eng Chem Res 2003, 42, 6431.
12. Alsoy, S.; Duda, J. L. Chem Eng Tech 1999, 22, 971.
13. Woods, H. M.; Silva, M. M.; Nouvel, C.; Shakesheff, K. M.; Howdle, S. M. J Mater Chem 2004, 14, 1663.
14. Garcia, L. M.; Lesser, A. J. J Appl Polym Sci 2004, 93, 1501.

15. Beckman, E. J. Ind Eng Chem Res 2003, 42, 1598.
16. Liu, T.; Hu, G. H.; Tong, G. Sh.; Zhao, L.; Cao, G. P.; Yuan, W. K. Ind Eng Chem Res 2005, 44, 4292.
17. Li, B.; Cao, G. P.; Liu, T.; Zhao, L.; Yuan, W. K.; Hu, G. H. Chin J Chem Eng 2005, 13, 673.
18. Berens, A. R.; Huvard, G. S.; Korsmeyer, R. W.; Kunig, F. W. J Appl Polym Sci 1992, 46, 231.
19. Dorazio, L.; Mancarella, C.; Martuscelli, E.; Sticotti, G. J Mater Sci 1991, 26, 4033.
20. Dogopolsky, I.; Silberman, A.; Kenig, S. Polym Adv Technol 1995, 6, 653.
21. Avalos, F.; Lopez-Manchado, M. A.; Arroyo, M. Polymer 1996, 37, 5681.
22. Yokoyama, Y.; Ricco, T. J Appl Polym Sci 1997, 66, 1007.
23. Miteva, T.; Minkova, L.; Magagnini, P. Macromol Chem Phys 1998, 199, 1519.
24. Tjong, S. C.; Xu, S. A. Polym Int 1997, 44, 95.
25. Iroh, J. O.; Berry, J. P. Polymer 1993, 34, 4747.
26. Binsbergen, F. L.; de Lange, B. G. M. Polymer 1968, 9, 23.
27. Progelhof, R. C.; Throne, J. L. Polymer Engineering Principles; Academic Press: New York, 1993; pp 95–150, .
28. Seo, Y. S.; Kim, J. H.; Kim, K. U. Polymer 2000, 41, 2639.